

# Intermediate tunnelling–hopping regime in DNA charge transport

Limin Xiang<sup>1,2</sup>, Julio L. Palma<sup>1,2</sup>, Christopher Bruot<sup>1</sup>, Vladimiro Mujica<sup>2</sup>, Mark A. Ratner<sup>3</sup> and Nongjian Tao<sup>1,4\*</sup>

**Charge transport in molecular systems, including DNA, is involved in many basic chemical and biological processes, and its understanding is critical if they are to be used in electronic devices. This important phenomenon is often described as either coherent tunnelling over a short distance or incoherent hopping over a long distance. Here, we show evidence of an intermediate regime where coherent and incoherent processes coexist in double-stranded DNA. We measure charge transport in single DNA molecules bridged to two electrodes as a function of DNA sequence and length. In general, the resistance of DNA increases linearly with length, as expected for incoherent hopping. However, for DNA sequences with stacked guanine–cytosine (GC) base pairs, a periodic oscillation is superimposed on the linear length dependence, indicating partial coherent transport. This result is supported by the finding of strong delocalization of the highest occupied molecular orbitals of GC by theoretical simulation and by modelling based on the Büttiker theory of partial coherent charge transport.**

Charge transport and related charge transfer processes in double helical DNA have received ongoing interest over recent decades because of their relevance to the oxidative damage to DNA, which is critical to the viability of all living organisms<sup>1,2</sup>. The observation of long-range charge transport in DNA<sup>3,4</sup> and advances in synthesizing DNA with defined nanostructures<sup>5</sup> have further stimulated research interest in exploring DNA as a building block for nanoelectronic applications. Both unravelling the oxidative damage seen in DNA and building functional electronic devices with DNA require a better understanding of the charge transport mechanism in DNA.

Charge transport and transfer processes in DNA have been studied using a range of experimental methods<sup>3,6–14</sup>, theoretical models<sup>15–17</sup> and computer simulations<sup>18–20</sup>. Coherent tunnelling and incoherent hopping have emerged as the mainstream theories to explain short-range and long-range charge transport in DNA<sup>21</sup>, respectively. In the tunnelling regime, the resistance increases exponentially with molecular length<sup>15</sup>, whereas in the hopping regime the resistance increases linearly with length<sup>16</sup>. In the model of incoherent hopping in DNA, each purine base is treated as a hopping site for a hole. However, a recent simulation has shown that strong electronic coupling between the  $\pi$ -electrons of neighbouring base pairs can lead to delocalization of the holes over several base pairs in DNA hairpins<sup>18</sup>, suggesting a role of coherence in the hopping regime.

Here, we report direct experimental evidence for an intermediate regime—distinctly different from the simple coherent tunnelling and incoherent hopping mechanisms alone—by studying charge transport in double-helical DNA bridged between two electrodes in an aqueous solution (Fig. 1a). Unlike previous work<sup>10</sup> we connected the electrodes directly to the DNA bases, thereby providing efficient electronic coupling between the electrodes and DNA. To maximize the electronic coupling between the  $\pi$ -electrons of neighbouring base pairs<sup>22,23</sup>, we selected DNA sequences with guanine (G) bases stacked on top of one another. Although the overall resistance increased linearly with molecular length, as expected for hopping transport, we observed a periodic oscillation superimposed

on the linear dependence. This has been found to be a signature of electron (or hole) delocalization in metallic wires<sup>24</sup> or other conjugate systems<sup>25</sup>, originating from quantum confinement and scattering by the two ends of the wires. As a control experiment, we also measured DNA sequences with alternating G (in which the G bases do not stack on top of one another), and found that the resistance increases linearly with molecular length, in agreement with the hopping model. We attribute the observed resistance oscillation to delocalization of holes induced by the strong electronic coupling between stacked G bases. We further describe the experimental results with a model based on the concept introduced by Büttiker<sup>26</sup>, which allows the coexistence of a partial coherence mechanism and incoherent hopping transport.

## Results and discussions

We focus on DNA sequences with stacked G bases because G has the lowest ionization potential of the four DNA bases (A, T, G and C)<sup>27</sup>, so the highest occupied molecular orbital (HOMO) levels are closest to the electrode Fermi level<sup>28</sup>. More importantly, both theoretical and experimental results have shown that G doublets (GG) and triplets (GGG) have lower ionization potentials than a single G<sup>29,30</sup>, indicating strong coupling between the  $\pi$  orbitals of the G, leading to strong delocalization of holes<sup>11,17,18</sup>. The stacked-G DNA sequences studied here are denoted 5'-AC<sub>n</sub>G<sub>n</sub>T-3' ( $n = 3, 4, 5, 6, 7, 8$ ), and the alternating G sequences are denoted 5'-A(CG)<sub>n</sub>T-3' ( $n = 3, 4, 5, 6, 7$ ), where A, G, C and T indicate adenine, guanine, cytosine and thymine, respectively. Both sets of DNA are double-stranded and self-complementary, so the complementary sequences also include alternating and stacked G bases respectively.

Direct electrical measurement of DNA requires a good contact between the molecule and the probing electrodes. In our previous work<sup>10</sup> we connected the electrodes to the sugar group of the DNA. However, because charge transport in DNA is dominated by the overlap of the  $\pi$  orbitals of the stacked base pairs<sup>31</sup>, the present work introduces a linker (amine<sup>32</sup>) on T (Fig. 1a) to minimize the contact resistance between the electrodes and DNA.

<sup>1</sup>Center for Biosensors and Bioelectronics, Biodesign Institute, Arizona State University, Tempe, Arizona 85287, USA. <sup>2</sup>Department of Chemistry and Biochemistry, Arizona State University, Tempe, Arizona 85287, USA. <sup>3</sup>Department of Chemistry, Northwestern University, Evanston, Illinois 60208, USA. <sup>4</sup>School of Electrical, Computer and Energy Engineering, Arizona State University, Tempe, Arizona 85287, USA. \*e-mail: njtao@asu.edu

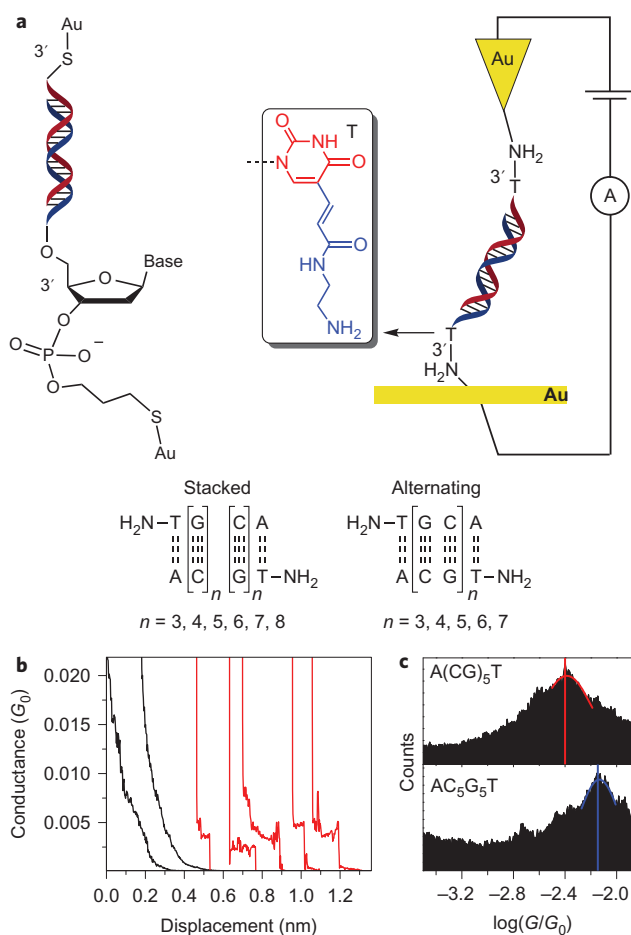


**Figure 1 | Direct measurement of charge transport in dsDNA attached to two electrodes.** **a**, DNA molecules connected to two electrodes via the sugar<sup>10</sup> (left) and directly via the thymine base (T, right). The red part of the chemical scheme is the original T base, and the blue part is the amine modification. Note that  $A(CG)_nT$  and  $AC_nG_nT$  denote alternating and stacked G sequences, respectively. **b**, Representative current–distance traces (current has been converted to conductance) of  $A(CG)_5T$  (red lines) in aqueous solution, showing plateau features in the traces, and control experiments performed in the absence of DNA molecules showing perfect exponential decay (black lines). **c**, Conductance histograms of  $A(CG)_5T$  and  $AC_5G_5T$  constructed from thousands of individual traces, then fitted by a Gaussian distribution function; peak positions (red and blue lines) indicate conductance values for the molecules.

Charge transport measurements were performed using a scanning tunnelling microscope (STM) break-junction technique<sup>33,34</sup>. A gold tip was coated with a wax insulation layer, thereby reducing the ionic leakage current to below 1 pA (ref. 10). The tip was repeatedly brought into and out of contact with a gold substrate covered with DNA molecules to create Au–DNA–Au junctions (Fig. 1a). During the pulling process the current was recorded versus distance, and a step in the current indicated the formation of a DNA molecule bridged between the substrate and tip electrodes (Fig. 1b). Thousands of current–distance traces were collected for each DNA sample, from which a conductance histogram was constructed. Figure 1c presents the conductance histograms of 5′- $A(CG)_5T$ -3′ and 5′- $AC_5G_5T$ -3′. From the peak positions of the histograms, the most probable conductance values of the two DNA sequences were obtained.

Figure 2a plots the resistance (inverse of conductance) as a function of DNA length for both the stacked G (blue triangles) and the alternating G (black squares) DNA sequences (Table 1). The stacked

and alternating G DNA molecules differ only in their sequence order, but their charge transport behaviours are significantly different. First, for the same length, the stacked G sequence is more conductive (or less resistive) than the corresponding alternating sequence. Second, the overall resistance of both the stacked and alternating G sequences increases linearly with length, which is expected for hopping<sup>35,36</sup>, but the slope of the resistance versus length plot for the stacked G DNA is smaller than the alternating G DNA. In other words, the conductance of the stacked G DNA sequences depends on the length more weakly. The most striking observation is a distinct oscillation of resistance superimposed on the linear increase of resistance with length for the stacked G DNA sequences. Finally, we compared the conductance of the DNA when the electrode is connected to the base with the conductance when the electrode is connected to the sugar group (Fig. 1a). We discuss each of the above observations in the following.

**Linear dependence of DNA resistance with length in alternating sequences.** Let us first examine the relative conductivities of the alternating and stacked G sequences by analysing the relative energy level alignment and delocalization of holes in both sequences. Figure 2b presents three-dimensional structures of alternating and stacked G sequences of the canonical B-DNA double helix, clearly showing the dramatic difference in the stacking of G bases in the two DNA sequences. In the alternating case, nearest-neighbour G bases do not overlap with each other directly, in contrast to the

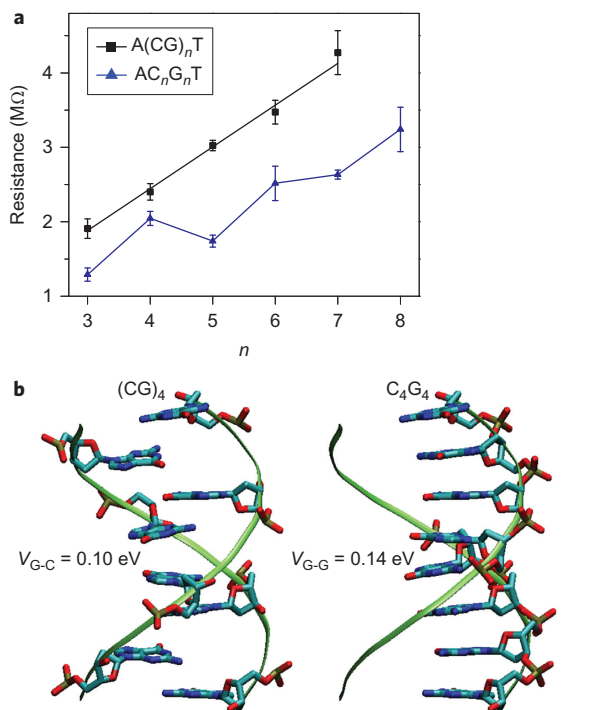


**Figure 2 | Resistance and structure of alternating ( $A(CG)_nT$ ) and stacked ( $AC_nG_nT$ ) G DNA sequences.** **a**, Resistance of alternating (black squares) and stacked (blue triangles) G DNA sequences versus the number of CG in the sequences. The stacked sequences have smaller resistance values than alternating sequences, and an oscillation is superimposed on the linear trend. Error bars are standard deviations calculated from three to four sets of experiments for each individual sequence (Supplementary Table 1). **b**, Three-dimensional structures of alternating ( $(CG)_4$ , left) and stacked ( $C_4G_4$ , right) G dsDNA, showing a better overlap between adjacent G bases for stacked G sequences than alternating sequences. This is also supported by the calculated electronic couplings at the INDO/S level between adjacent base pairs, indicated as  $V_{G-C}$  for the alternating sequence and  $V_{G-G}$  for the stacked sequence.

**Table 1 | Conductance values and peak width for alternating A(CG)<sub>n</sub>T and stacked AC<sub>n</sub>G<sub>n</sub>T sequences obtained by fitting the peaks in the histograms.**

| Alternating sequences | Peak position* log(G/G <sub>0</sub> ) | Peak width | Stacked sequences                | Peak position log(G/G <sub>0</sub> ) | Peak width |
|-----------------------|---------------------------------------|------------|----------------------------------|--------------------------------------|------------|
| A(CG) <sub>3</sub> T  | -2.17 ± 0.03                          | 0.22       | AC <sub>3</sub> G <sub>3</sub> T | -2.00 ± 0.03                         | 0.36       |
| A(CG) <sub>4</sub> T  | -2.27 ± 0.02                          | 0.20       | AC <sub>4</sub> G <sub>4</sub> T | -2.20 ± 0.02                         | 0.33       |
| A(CG) <sub>5</sub> T  | -2.37 ± 0.01                          | 0.21       | AC <sub>5</sub> G <sub>5</sub> T | -2.13 ± 0.02                         | 0.16       |
| A(CG) <sub>6</sub> T  | -2.43 ± 0.02                          | 0.36       | AC <sub>6</sub> G <sub>6</sub> T | -2.29 ± 0.04                         | 0.21       |
| A(CG) <sub>7</sub> T  | -2.52 ± 0.03                          | 0.28       | AC <sub>7</sub> G <sub>7</sub> T | -2.31 ± 0.01                         | 0.23       |
|                       |                                       |            | AC <sub>8</sub> G <sub>8</sub> T | -2.40 ± 0.04                         | 0.23       |

\*Error bars are calculated from three to four sets of experiments for each individual sequence (Supplementary Table 1).

stacked case, where the nearest-neighbour G bases stack on top of one another, leading to a stronger electronic coupling between the adjacent G bases<sup>22,23</sup>. This is validated by our electronic coupling calculations based on the INDO/S Hamiltonian, which show that the coupling coefficients between neighbouring G bases are 0.10 eV and 0.14 eV for alternating and stacked sequences, respectively. The strong electronic coupling in the stacked G DNA molecules also indicates that holes can delocalize over several neighbouring G bases, thus creating a higher HOMO level<sup>28</sup>.

We also calculated the HOMO levels or ionization potentials of the stacked G DNA sequences (Supplementary Fig. 10), and found that they vary as follows: G (-7.75 eV), GC (-7.24 eV), G<sub>2</sub>C<sub>2</sub> (-6.61 eV), G<sub>3</sub>C<sub>3</sub> (-6.30 eV), G<sub>4</sub>C<sub>4</sub> (-6.15 eV), G<sub>5</sub>C<sub>5</sub> (-6.07 eV) and G<sub>6</sub>C<sub>6</sub> (-6.01 eV). These values are consistent with results reported in the literature. For example, Saito and colleagues<sup>29</sup> concluded that the GGG moiety was easier to oxidize than G, based on a photoinduced DNA cleavage measurement, while Ratner and co-workers<sup>30</sup> reported that the ionization potentials of GG and GGG were lower than G by 0.5 and 0.7 eV, respectively. These experimental and theoretical studies all show that the HOMO energy levels of stacked G sequences are closer to the Fermi energy level of the electrode due to delocalization.

The linear increase in the DNA resistance with length is a signature of hopping transport<sup>35,36</sup>. When applying the hopping model to DNA, it is often assumed implicitly that each G is a hopping site, and holes hop along the individual hopping sites from the left electrode to the right electrode<sup>16</sup> (Fig. 3, top). In alternating G DNA molecules, the molecular orbitals near the Fermi levels are localized mainly on a single G base (Fig. 3, bottom; Supplementary Fig. 7), which

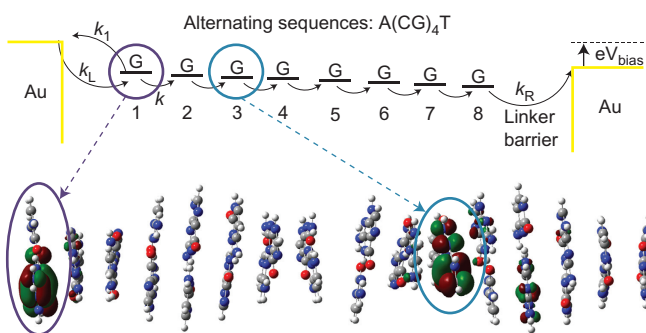


**Figure 3 | Hopping transport in alternating G DNA sequences.** Holes from the left electrode migrate through each of the hopping sites and finally reach the right electrode, generating a current when a small bias  $V_{\text{bias}}$  is applied between the left and right electrodes.  $k_L$ ,  $k_R$  and  $k$  are the hole transfer rate constants from the left electrode to the first G of the DNA, from the first G back to the left electrode, from the last G of the DNA to the right electrode, and between adjacent hopping sites, respectively. The HOMOs of the G bases, which are responsible for hole hopping, are strongly localized in single G bases, and the corresponding energy levels are degenerate, which indicates that each of the G bases in the dsDNA is a hopping site. Note that (CG)<sub>4</sub> is shown here as an example.

supports the notion that each G base acts as a hopping site. The resistance of the DNA molecule is proportional to the inverse of the charge transport rate  $k_{\text{CT}}$ , and is given by  $R = [e^2 k_{\text{CT}} \rho(E_F)]^{-1}$  (ref. 37), where  $e$  is the elementary charge and  $\rho(E_F)$  is the density of states at the Fermi level. According to a sequential hopping model based on the steady-state flux method, the resistance is described by<sup>37,38</sup>

$$R = \frac{k_L^{-1} + k_R^{-1}}{e^2 \rho(E_F)} e^{E_a/k_B T} + \frac{N-1}{e^2 \rho(E_F)} k^{-1} e^{E_a/k_B T} \quad (1)$$

where  $k_L$ ,  $k_R$  and  $k$  are the hole transfer rate constants from the left electrode to the first G of the DNA, from the last G of the DNA to the right electrode and between adjacent hopping sites, respectively,  $E_a$  is the activation energy,  $k_B$  is the Boltzmann constant, and  $T$  is temperature. The first term in equation (1) represents the electrode-molecule contact resistance, and the second term describes the efficiency of hole hopping along the DNA. By fitting the length dependence of resistance with equation (1), the slopes for the alternating and stacked G DNA sequences are  $0.56 \pm 0.05 \text{ M}\Omega$  and  $0.31 \pm 0.01 \text{ M}\Omega$ , respectively, corresponding to a ratio of 1.8 between the two slopes. According to Marcus theory, the charge transfer rate is proportional to the square of the coupling. The square of the calculated ratio of the electronic coupling strengths between the stacked and alternating G DNA sequences is  $\sim 1.4^2 = 1.96$ , which is consistent with the observed ratio of the slopes.

**Periodic oscillation of DNA resistance with length in stacked sequences.** The puzzling observation is the periodic oscillation in the resistance versus length plot for the stacked G DNA sequences, which cannot be described by the hopping model. Periodic oscillations in the length dependence of resistance have been observed previously in coherent transport in systems such as one-dimensional atomic wires<sup>24</sup>, and are predicted for one-dimensional conjugated molecular systems involving strong overlap of  $\pi$  electrons<sup>25</sup>. By assuming coherent resonant tunnelling, periodic oscillation in the resistance of DNA molecules has also been predicted<sup>19</sup>. However, in those coherent transport systems the overall resistance varies little with length, in contrast with the present observation in stacked G DNA sequences. Another observation that is not predicted by the simple coherent transport model is that the oscillation amplitude decreases with molecular length.

The origin of the resistance oscillation in one-dimensional metallic wires and conjugated molecular systems is delocalization of electrons in such systems. The electrons are reflected by boundaries and form standing waves<sup>24</sup>. In stacked G DNA molecules, the occupied molecular orbitals are delocalized over two to three base pairs, and their energy levels are close to the Fermi level of the electrodes (Fig. 4 and Supplementary Fig. 8). In other words, in contrast to the alternating G DNA sequences, where each hopping site is a G base, the hopping site in the stacked G sequences consists of two to three base pairs (Fig. 4a). This delocalization domain has been reported previously by Barton and colleagues<sup>39</sup> for charge transfer through stacked A domains, and by Majima and colleagues<sup>11</sup> for charge

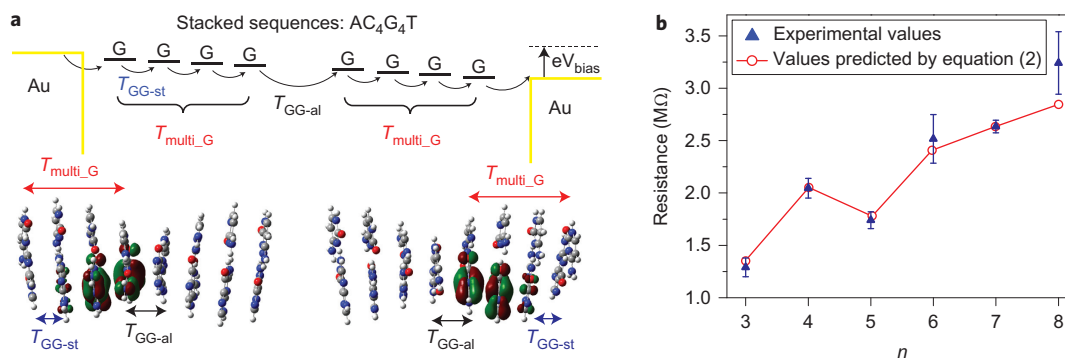


**Figure 4 | Intermediate tunnelling-hopping charge transport in stacked DNA sequences.** **a**, Top: schematic of the intermediate tunnelling-hopping transport mechanism in stacked sequences, where  $T_{\text{multi-G}}$  is the probability of transmission via the stacked G-segments of the DNA including the coherent correction,  $T_{\text{GG-st}}$  is the probability of transmission between two adjacent stacked Gs, and  $T_{\text{GG-al}}$  is the probability of transmission between the two stacked G-segments.  $T_{\text{GG-st}}$  and  $T_{\text{GG-al}}$  have incoherent components only. Bottom: HOMO levels of  $C_4G_4$  show delocalization of the orbitals, in contrast to Fig. 3, indicating that the coherent tunnelling transport coexists with incoherent hopping transport through the stacked G-segments. Note that, as for alternating sequences, there is no delocalization between the fourth G and fifth G in the middle. **b**, Experimental resistance (blue triangles) and prediction of Büttiker theory (see equation (2)) of partial coherent charge transport (red circles), indicating that the oscillation is caused by coherent processes when holes transport through stacked G-segments. Error bars are standard deviations calculated from three to four sets of experiments for each individual sequence (Supplementary Table 1).

transfer in DNA sequences containing stacked GAG bases. The former reported a periodicity in the charger transfer yield versus length, and the latter showed an oscillation depending on the position of the delocalization region (stacked GAG) along the helix. The delocalization of holes over multiple bases suggests that the coherency of holes does not become fully washed out over a short distance, and the sequential hopping model must be modified to include this feature. This conclusion is consistent with the theory of Renaud and colleagues<sup>18</sup> for poly(A)-poly(T) DNA hairpins, and the theoretical analysis by Venkatramani and co-workers<sup>40</sup> for peptide nucleic acids and de Pablo *et al.*<sup>14</sup> for  $\lambda$ -DNA. We also note that coherent superexchange is considered in the variable range hopping model of charge transfer in DNA developed by Yu and colleagues<sup>41</sup> and Renger and colleagues<sup>42</sup> (see Supplementary Fig. 9 for further discussions).

Partially coherent and incoherent charge transport has been studied in semiconductor devices. Büttiker<sup>26</sup> developed a theory that includes a coherent correction to the completely incoherent charge transport in one-dimensional systems. Here, we apply that theory to describe charge transport in stacked G DNA sequences (Fig. 4a), and find that the total resistance of the DNA can be expressed as

$$R_{\text{tot}} = R_0 + \frac{h}{e^2} \frac{N-1}{1 - 2e^{-B(N-1)} \cos[C(N-1)]} T_{\text{GG-st}}^{-1} \quad (2)$$

where the first term,  $R_0$ , is the contact resistance (including hopping between the two stacked G regions in the middle of the molecule, described by  $T_{\text{GG-al}}$  in Fig. 4a), and the second term describes hopping with a coherent transport correction. In equation (2),  $T_{\text{GG-st}}$  is the probability of transmission from one G to an adjacent G,  $B = w_0/v\tau_i$  reflects the decay of coherence over distance ( $v\tau_i$  is the coherence length), where  $v$  is the velocity of the carrier,  $\tau_i$  is the inelastic scattering time, and  $w_0 = 3.32 \text{ \AA}$  is the base pair distance in B-form poly GC DNA<sup>43</sup>,  $C = (2\sqrt{2mE})/\hbar w_0$ , where  $m = 1.68 m_e$  (ref. 43) and  $E$  are the mass and energy of the holes, respectively. Note that equation (2) is similar to equation (1) except for the denominator in the second term of equation (2), which is the contribution of coherent transport introduced by Büttiker<sup>26</sup>, leading to a periodic oscillation in the length dependence of the resistance.

Figure 4b shows the fit of the experimental data (blue triangles) to the model (red circles) given by equation (2). The contact resistance  $R_0$  was preset as  $0.76 \text{ M}\Omega$ , which was obtained by extrapolating the length dependence of the resistance to the  $A(\text{CG})_1\text{T}$  sequence for the alternating sequence. From the fitting, the resistance per GC base pair is  $0.31 \pm 0.01 \text{ M}\Omega$ . The energy of the holes calculated from the fitting parameter  $C$  is  $0.29 \pm 0.02 \text{ eV}$ .  $v\tau_i$  is  $0.56 \pm 0.06 \text{ nm}$ , which gives a coherence length of approximately two base pairs, consistent with other experimental work<sup>12,44</sup> and theoretical prediction<sup>18,45</sup> for charge transport through stacked A sequences. The experimental data can be accurately described with the Büttiker theory with reasonable physical parameters (see Supplementary Figs 11 and 12 for further discussions), which supports the conclusion of partial coherent and incoherent transport in stacked G bases.

To further validate the oscillation behaviour in the stacked G sequences, we performed conductance measurements on  $AC_nG_n\text{T}$  ( $n = 3, 4, 5, 6$ ) sequences with the electrode connected to the sugar group of the DNA (Supplementary Fig. 5). The oscillation behaviour still exists, but with a smaller amplitude. We note that the oscillation behaviour is rarely seen in other  $\pi$ -conjugated systems<sup>46</sup>. The molecular energy levels in these  $\pi$ -conjugated systems are far away from the Fermi level of the electrodes, so coherent tunnelling is the dominant transport mechanism, leading to an exponential increase in the resistance with length. In DNA, thermal activation helps bring the HOMO to the Fermi level, and holes are injected into the DNA<sup>16</sup>. We expect this oscillatory transport to occur in other conjugate systems if the molecular energy levels can be brought to align with the Fermi level, either with a gate control or thermal activation.

**Table 2 | Conductance values and peak width for the alternating sequences  $A(\text{CG})_n\text{T}$  with amine on thymine and thiol on the sugar group.**

| Contact via DNA base     | Peak position $\log(G/G_0)$ | Peak width | Contact via sugar group* | Peak position $\log(G/G_0)$ |
|--------------------------|-----------------------------|------------|--------------------------|-----------------------------|
| $A(\text{CG})_3\text{T}$ | $-2.17 \pm 0.03$            | 0.22       | $(\text{CG})_4$          | -2.89                       |
| $A(\text{CG})_4\text{T}$ | $-2.27 \pm 0.02$            | 0.20       | $(\text{CG})_5$          | -3.10                       |
| $A(\text{CG})_5\text{T}$ | $-2.37 \pm 0.01$            | 0.21       | $(\text{CG})_6$          | -3.22                       |
| $A(\text{CG})_6\text{T}$ | $-2.43 \pm 0.02$            | 0.36       | $(\text{CG})_7$          | -3.40                       |

\*See conductance values in ref. 10.

To examine the DNA–electrode contact effect (Fig. 1a) we compared the conductance values measured here with those obtained with the electrode connected to the sugar group of the DNA<sup>10</sup> (Table 2). The data show that the contact via the DNA base in the present work is three to six times more conductive than the sugar contact. This observation supports that charge transport in DNA is mainly via the base pairs<sup>31</sup>.

## Conclusions

We have studied charge transport in DNA duplexes with alternating G and stacked G sequences. In the former, the resistance increases linearly with molecular length (number of base pairs), which can be described with the hopping model, in which each G base acts as a hopping site. In the latter case the overall resistance also follows the linear length dependence trend, but there is a surprising periodic oscillation superimposed on the linear dependence, indicating a partially coherent and partially hopping regime of charge transport. Our calculations reveal that the HOMOs in the stacked G are delocalized over several G bases, supporting the observation of an intermediate coherent tunnelling and incoherent hopping charge transport mechanism. The experimental resistance versus length dependence can be modelled based on Büttiker theory, which includes partial coherence in incoherent hopping. The present work also shows that connecting the electrodes to the DNA base pairs provides more efficient electrical contact to the molecule than when connecting to the DNA via the sugar group.

## Methods

**Sample preparation.** All DNA samples were purchased from Bio-Synthesis (HPLC-purified with a certificate of analysis via mass spectroscopy). Na<sub>2</sub>HPO<sub>4</sub>·2H<sub>2</sub>O (for HPLC, ≥98.5%) and NaH<sub>2</sub>PO<sub>4</sub> (for HPLC, ≥99.0%) were purchased from Fluka, and Mg(OAc)<sub>2</sub> (ACS reagent, 99.5–102%) was purchased from Sigma-Aldrich. All reagents were used without further purification. A Multigene Mini Thermal Cycler (model TC-050-18) was used to anneal DNA solution samples. Phosphate buffer (pH 7.0) was prepared by dissolving Na<sub>2</sub>HPO<sub>4</sub>·2H<sub>2</sub>O (198 mg), NaH<sub>2</sub>PO<sub>4</sub> (133 mg) and Mg(OAc)<sub>2</sub> (47 mg) in 10 ml deionized water. Double-stranded DNA (dsDNA) solution was prepared by mixing 90 µl phosphate buffer with 10 µl of 100 µM single-stranded DNA (ssDNA) solution (dissolved in deionized water) and annealed by varying the temperature from 80 °C to 8 °C over a period of 4 h (kept at a certain temperature for 3 min and 20 s, then decreasing the temperature by 1 °C), and then kept at 4 °C. The annealing process for longer-strand DNA ( $n \geq 6$ ) comprised 5 min at 95 °C, cooling from 95 °C to 90 °C at the rate of 4 °C per second, cooling from 90 °C to 76 °C at a rate of 1 °C per 5 min, further cooling from 76 °C to 26 °C at a rate of 1 °C per 15 min, holding at 25 °C for 30 min, then maintained at 4 °C. This stepwise process helped prevent the formation of ssDNA hairpin structures. For further details see Supplementary Figs 1 and 2. All other experiment set-ups are described in previous reports<sup>10</sup>.

**Conductance measurement method.** Measurements were carried out in a 2.5 µM dsDNA solution at room temperature (22 °C). Phosphate buffer (50 µl) was added into the sample holder. A small bias voltage (10 mV to 30 mV, positive or negative, see Supplementary Table 1) was applied between the gold tip and the gold substrate in an STM break-junction set-up. An exponential decay in the current–distance traces was observed in the phosphate buffer in the absence of DNA molecules (black traces in Fig. 1b). However, after adding 50 µl dsDNA solution of 5 µM, steps appeared (red traces in Fig. 1b). A large number of current–distance traces (~5,000) were recorded for each experiment, and conductance histograms were constructed with an algorithm (described previously<sup>47</sup>). The algorithm counted only the traces showing counts exceeding a preset threshold in the histograms (Fig. 1b). For each sequence, the measurement was repeated three to four times on different days. In addition to pure phosphate buffer, measurements were also carried out in ssDNA solution as a further control experiment. The absence of steps in the current–distance traces with ssDNA indicates no hairpin formation in the samples (Supplementary Figs 3 and 4). Individual current–voltage ( $I$ – $V$ ) curves were also recorded for A(CG) <sub>$n$</sub> T and AC <sub>$n$</sub> G <sub>$n$</sub> T sequences (Supplementary Fig. 6). The  $I$ – $V$  curves are symmetric, indicating a symmetric contribution of the contacts to the charge transport measured with the STM break-junction method.

**Theoretical calculation method.** We performed quantum-chemical calculations to obtain orbital energies at equilibrium (zero bias) of the dsDNA sequences at the INDO/S level with a minimal basis set, which has been shown to be a reliable method for the description of electronic coupling between base pairs of DNA<sup>48</sup>. Electronic coupling calculations were performed under the two-state model<sup>48</sup> framework with the systems set at the conformation of canonical B-DNA and only the base pairs were considered (the backbone was removed). We used two

neighbouring stacked base pairs and approximated the donor and acceptor states by the HOMO orbitals of each Watson–Crick base pair in the presence of the neighbouring base pair, and used the Hamiltonian in the basis of atomic orbitals to obtain the coupling coefficient (Supplementary Section 7).

Received 20 October 2014; accepted 14 January 2015;  
published online 20 February 2015

## References

- Wallace, S. S. Biological consequences of free radical-damaged DNA bases. *Free Radic. Bio. Med.* **33**, 1–14 (2002).
- Kawanishi, S., Hiraku, Y. & Oikawa, S. Mechanism of guanine-specific DNA damage by oxidative stress and its role in carcinogenesis and aging. *Mutat. Res. Rev. Mutat.* **488**, 65–76 (2001).
- Murphy, C. J. *et al.* Long-range photoinduced electron-transfer through a DNA helix. *Science* **262**, 1025–1029 (1993).
- Giese, B. Long-distance charge transport in DNA: the hopping mechanism. *Acc. Chem. Res.* **33**, 631–636 (2000).
- Seeman, N. C. Nanomaterials based on DNA. *Annu. Rev. Biochem.* **79**, 65–87 (2010).
- Lewis, F. D. *et al.* Distance-dependent electron transfer in DNA hairpins. *Science* **277**, 673–676 (1997).
- Kelley, S. O., Jackson, N. M., Hill, M. G. & Barton, J. K. Long-range electron transfer through DNA films. *Angew. Chem. Int. Ed.* **38**, 941–945 (1999).
- Porath, D., Bezryadin, A., de Vries, S. & Dekker, C. Direct measurement of electrical transport through DNA molecules. *Nature* **403**, 635–638 (2000).
- Fink, H.-W. & Schonberger, C. Electrical conduction through DNA molecules. *Nature* **398**, 407–410 (1999).
- Xu, B. Q. *et al.* Direct conductance measurement of single DNA molecules in aqueous solution. *Nano. Lett.* **4**, 1105–1108 (2004).
- Kawai, K. & Majima, T. Hole transfer kinetics of DNA. *Acc. Chem. Res.* **46**, 2616–2625 (2013).
- Giese, B., Amaudrut, J., Kohler, A.-K., Spormann, M. & Wessely, S. Direct observation of hole transfer through DNA by hopping between adenine bases and by tunnelling. *Nature* **412**, 318–320 (2001).
- Zalinger, H., Schiffrin, D. J., Bates, A. D., Straikov, E. B., Wenzel, W. & Nichols, R. J. Variable-temperature measurements of the single-molecule conductance of double-stranded DNA. *Angew. Chem. Int. Ed.* **45**, 5499–5502 (2006).
- de Pablo, P. J. *et al.* Absence of dc-conductivity in  $\lambda$ -DNA. *Phys. Rev. Lett.* **85**, 4992–4995 (2000).
- Risser, S. M., Beratan, D. N. & Meade, T. J. Electron transfer in DNA: predictions of exponential growth and decay of coupling with donor–acceptor distance. *J. Am. Chem. Soc.* **115**, 2508–2510 (1993).
- Jortner, J., Bixon, M., Langenbacher, T. & Michel-Beyerle, M. E. Charge transfer and transport in DNA. *Proc. Natl Acad. Sci. USA* **95**, 12759–12765 (1998).
- Conwell, E. M. Charge transport in DNA in solution: the role of polarons. *Proc. Natl Acad. Sci. USA* **102**, 8795–8799 (2005).
- Renaud, N., Berlin, Y. A., Lewis, F. D. & Ratner, M. A. Between superexchange and hopping: an intermediate charge-transfer mechanism in poly(A)–poly(T) DNA hairpins. *J. Am. Chem. Soc.* **135**, 3953–3963 (2013).
- Grib, N. V. Distance-dependent coherent charge transport in DNA: crossover from tunneling to free propagation. *J. Biophys. Chem.* **1**, 77–85 (2010).
- Zhang, Y., Liu, C., Balaeff, A., Skourtis, S. S. & Beratan, D. N. A flickering resonance mechanism for biological charge transfer. *Proc. Natl Acad. Sci. USA* **111**, 10049–10054 (2014).
- Genevieux, J. C. & Barton, J. K. Mechanisms for DNA charge transport. *Chem. Rev.* **110**, 1642–1662 (2009).
- Voityuk, A. A., Rösch, N., Bixon, M. & Jortner, J. Electronic coupling for charge transfer and transport in DNA. *J. Phys. Chem. B* **104**, 9740–9745 (2000).
- Šponer, J., Leszczyński, J. & Hobza, P. Nature of nucleic acid–base stacking: nonempirical *ab initio* and empirical potential characterization of 10 stacked base dimers. Comparison of stacked and H-bonded base pairs. *J. Phys. Chem.* **100**, 5590–5596 (1996).
- Smit, R. H. M., Untiedt, C., Rubio-Bollinger, G., Segers, R. C. & van Ruitenbeek, J. M. Observation of a parity oscillation in the conductance of atomic wires. *Phys. Rev. Lett.* **91**, 076805 (2003).
- Tada, T., Nozaki, D., Kondo, M., Hamayama, S. & Yoshizawa, K. Oscillation of conductance in molecular junctions of carbon ladder compounds. *J. Am. Chem. Soc.* **126**, 14182–14189 (2004).
- Büttiker, M. Coherent and sequential tunneling in series barriers. *IBM J. Res. Dev.* **32**, 63–75 (1988).
- Hush, N. S. & Cheung, A. S. Ionization potentials and donor properties of nucleic acid bases and related compounds. *Chem. Phys. Lett.* **34**, 11–13 (1975).
- Di Felice, R., Calzolari, A., Molinari, E. & Garbesi, A. *Ab initio* study of model guanine assemblies: the role of coupling and band transport. *Phys. Rev. B* **65**, 045104 (2001).

29. Saito, I. *et al.* Photoinduced DNA cleavage via electron transfer: demonstration that guanine residues located 5' to guanine are the most electron-donating sites. *J. Am. Chem. Soc.* **117**, 6406–6407 (1995).
30. Berlin, Y. A., Burin, A. L. & Ratner, M. A. Charge hopping in DNA. *J. Am. Chem. Soc.* **123**, 260–268 (2000).
31. Liu, T. & Barton, J. K. DNA electrochemistry through the base pairs not the sugar–phosphate backbone. *J. Am. Chem. Soc.* **127**, 10160–10161 (2005).
32. Venkataraman, L. *et al.* Single-molecule circuits with well-defined molecular conductance. *Nano. Lett.* **6**, 458–462 (2006).
33. Xu, B. & Tao, N. J. Measurement of single-molecule resistance by repeated formation of molecular junctions. *Science* **301**, 1221–1223 (2003).
34. Haiss, W. *et al.* Redox state dependence of single molecule conductivity. *J. Am. Chem. Soc.* **125**, 15294–15295 (2003).
35. McCreery, R. Molecular electronic junctions. *Chem. Mater.* **16**, 4477–4496 (2004).
36. Luo, L., Choi, S. H. & Frisbie, C. D. Probing hopping conduction in conjugated molecular wires connected to metal electrodes. *Chem. Mater.* **23**, 631–645 (2011).
37. Segal, D., Nitzan, A., Ratner, M. & Davis, W. B. Activated conduction in microscopic molecular junctions. *J. Phys. Chem. B* **104**, 2790–2793 (2000).
38. Nitzan, A. The relationship between electron transfer rate and molecular conduction 2. The sequential hopping case. *Isr. J. Chem.* **42**, 163–166 (2002).
39. O'Neil, M. A. & Barton, J. K. DNA charge transport: conformationally gated hopping through stacked domains. *J. Am. Chem. Soc.* **126**, 11471–11483 (2004).
40. Venkatramani, R. *et al.* Evidence for a near-resonant charge transfer mechanism for double-stranded peptide nucleic acid. *J. Am. Chem. Soc.* **133**, 62–72 (2010).
41. Yu, Z. G. & Song, X. Variable range hopping and electrical conductivity along the DNA double helix. *Phys. Rev. Lett.* **86**, 6018–6021 (2001).
42. Renger, T. & Marcus, R. A. Variable-range hopping electron transfer through disordered bridge states: application to DNA. *J. Phys. Chem. A* **107**, 8404–8419 (2003).
43. Bende, A., Bogár, F. & Ladik, J. Hole mobilities of periodic models of DNA double helices in the nucleosomes at different temperatures. *Chem. Phys. Lett.* **565**, 128–131 (2013).
44. Lewis, F. D., Zhu, H., Daublain, P., Cohen, B. & Wasielewski, M. R. Hole mobility in DNA A tracts. *Angew. Chem. Int. Ed.* **45**, 7982–7985 (2006).
45. Jortner, J., Bixon, M., Voityuk, A. A. & Rösch, N. Superexchange mediated charge hopping in DNA. *J. Phys. Chem. A* **106**, 7599–7606 (2002).
46. Chen, W. *et al.* Highly conducting  $\pi$ -conjugated molecular junctions covalently bonded to gold electrodes. *J. Am. Chem. Soc.* **133**, 17160–17163 (2011).
47. Guo, S., Hihath, J., Díez-Pérez, I. & Tao, N. Measurement and statistical analysis of single-molecule current–voltage characteristics, transition voltage spectroscopy, and tunneling barrier height. *J. Am. Chem. Soc.* **133**, 19189–19197 (2011).
48. Berlin, Y. A., Voityuk, A. A. & Ratner, M. A. DNA base pair stacks with high electric conductance: a systematic structural search. *ACS Nano* **6**, 8216–8225 (2012).

### Acknowledgements

The authors thank S. Jiang and H. Yan for help with PAGE gel experiments, and D.N. Beratan, N. Seeman, F.D. Lewis, Y. Berlin, A. Balaeff and M.R. Wasielewski for discussions. The authors also acknowledge financial support from the Office of Naval Research (N00014-11-1-0729).

### Author contributions

L.X. and C.B. performed the conductance measurement experiments. J.L.P. performed INDO calculations. M.A.R. and V.M. supervised the INDO calculations. N.T. proposed the Büttiker model analysis and supervised the experiments.

### Additional information

Supplementary information is available in the [online version](#) of the paper. Reprints and permissions information is available online at [www.nature.com/reprints](http://www.nature.com/reprints). Correspondence and requests for materials should be addressed to N.T.

### Competing financial interests

The authors declare no competing financial interests.